Temperature-modulated fluorescence tomography in a turbid media

Yuting Lin (林钰婷),[1,a)] Linden Bolisay,[2] Michael Ghijsen,[1] Tiffany C. Kwong,[1,2] and Gultekin Gulsen[1]
[1]*Tu and Yuen Center for Functional Onco Imaging, Department of Radiological Sciences, University of California, Irvine, California 92697, USA*
[2]*InnoSense LLC, 2531 West 237th Street, Suite 12, Torrance, California 90505, USA*

(Received 22 November 2011; accepted 5 January 2012; published online 15 February 2012)

High scattering in biological tissues makes fluorescence tomography inverse problem very challenging in thick medium. We describe an approach termed "temperature-modulated fluorescence tomography" that can acquire fluorescence images at focused ultrasound resolution. By utilizing recently emerged temperature sensitive fluorescence contrast agents, this technique provides fluorescence images with high resolution prior to any reconstruction process. We demonstrate that this technique is well suited to resolve small fluorescence targets located several centimeters deep in tissue. © *2012 American Institute of Physics*. [doi:10.1063/1.3681378]

The ill-posed and underdetermined nature of the inverse problem does not permit optical imaging in thick tissue with high resolution. The main reason is the strong tissue scattering, making direct light focusing infeasible beyond one transport mean free path.[1] As one of the optical imaging techniques, fluorescence tomography (FT) utilizes laser light to excite the fluorescence sources located deep in a medium. Once excited, these sources relax to their ground state in nanoseconds by emitting lower energy photons. While propagating towards the surface of the medium, these photons are subject to a vast amount of scattering events along the way. This makes the FT inverse problem exceptionally difficult, which is defined as the problem of recovering the fluorescence source distribution from the measured light intensities on the tissue surface. Accordingly, the resolution and quantitative accuracy of the reconstructed images are very low.[2] An intriguing solution to this problem is to induce periodic displacement of scattering particles and variation of the refractive index in the medium using a focused ultrasound field. Using this approach and scanning the focused ultrasound field over the probed medium, ultrasound modulated fluorescence tomography (UMFT) can enhance the resolution.[3,4] However, only a small fraction of the photons that travels through the focused ultrasound column can be modulated at a time. The low modulation efficiency and extremely low signal to noise ratio (SNR) are the two main factors that make its implementation difficult. Recently, micro-bubbles that are surface-loaded with self quenching fluorophores are used to enhance the contrast of UMFT.[5,6] However, the main disadvantage of microbubbles are their instability, low circulation residence times, low binding efficiency to the area of interest especially in the fast-flow conditions, and possible side effects of their destruction during the imaging session.[7,8]

In this Letter, we present an approach that we termed "temperature-modulated fluorescence tomography (TM-FT)." TM-FT also utilizes focused ultrasound, which is rather used to heat the medium, only a couple of degree Celsius but with a high spatial resolution. A key element of the TM-FT is the recently emerged temperature-sensitive fluorescence contrast agents using ICG loaded pluronic nanocapsuless that pave the way for this technique.[9,10] The quantum efficiency of these nanocapsules was shown to be very sensitive to the temperature. For example, when heated from 22 to 40 °C, the fluorescence light intensity emitted by these nanocapsules increases two- to four-fold, and more importantly, this process is reversible. Our TM-FT technique leverages the temperature dependence of these contrast agents to overcome the spatial resolution limitation of conventional FT by using temperature modulation/tagging. In this technique, the medium is irradiated by both excitation light and a high intensity focused ultrasound (HIFU) wave. The crucial benefit of HIFU is that the temperature of the medium is modulated with very high spatial resolution (~1.5 mm) due to the absorption of acoustic power in the ultrasound focal zone. When the temperature sensitive fluorescence agents are present within the HIFU focal zone, local temperature increase affects their quantum efficiency. As a result, the emitted fluorescence light intensity has a substantial change. The difference in the detected fluorescence signal following the HIFU temperature modulation can render the position of these nanocapsules with high spatial resolution. Furthermore, this can be achieved without using a complex reconstruction algorithm as in the case for conventional FT.

To illustrate the TM-FT process for high resolution fluorescence tomography, the light propagation and heat transfer is modeled using a finite element method frame work. With diffusion approximation as the light propagation model in turbid medium, the TM-FT process is formulated with the following equations. Let us assume that the scanning area consists of discrete locations $[\vec{x}_i, i \le N]$. Equations (1) and (2) describe conditions before and after the application of the HIFU beam to obtain selectively localized heating in the medium, respectively,

$$-\nabla \cdot (D\nabla\varphi_0^m) + \mu_a\varphi_0^m = \eta(T_0)\mu_{af}\varphi^x \tag{1}$$

$$\text{and } -\nabla \cdot (D\nabla\varphi_i^m) + \mu_a\varphi_i^m = \eta(T_i)\delta(\vec{x}-\vec{x}_i)\mu_{af}\varphi^x,\ 1 \le i \le N \tag{2}$$

with the diffusion coefficient D, the absorption coefficient μ_a, the photon density at excitation (ϕ^x) and emission

a)Author to whom correspondence should be addressed. Electronic mail: yutingl@uci.edu. Tel.: 949-824-4176.

wavelength (ϕ^{m}), and the fluorescence absorption coefficient μ_{af}. The ideal focused heating at $\vec{x}_i$ corresponds to a delta function in Eq. (2), which can be approximated by a compactly supported and fast decaying function in practice. Let $d_i = \phi_{\mathrm{i}}^{\mathrm{m}} - \phi_0^{\mathrm{m}}$ and $\mathrm{c} = \eta(T_i) - \eta(T_0)$, we have:

$$-\nabla \cdot (D\nabla d_i) + \mu_a d_i = c\delta(\vec{x} - \vec{x}_i)\mu_{af}(\vec{x}_i)\varphi^x,\ 1 \le i \le N \quad (3)$$

The difference measurement d_i, only has values when the scanning step $\vec{x}_i$ is nonzero for $\mu_{af}(\vec{x}_i)$. Therefore, when the HIFU scans over the probed medium, the TM-FT could produce high resolution fluorescence images even without any reconstruction process.

We performed experimental studies to demonstrate that the TM-FT could penetrate several centimeters thick scattering tissue, still at ultrasound resolution (submillimeter to millimeter). The resolution of TM-FT mainly depends on the ultrasound transducer and achieving sub-milimeter resolution is possible using commercially available transducers. The schematic diagram of the system is shown in Fig. 1. A 785 nm laser diode (80 mW, Thorlabs, Newton, NJ) was used for fluorescence excitation. A network analyzer (Agilent Technologies, Palo Alto, CA) not only provided the RF modulation for the laser-diode but also measured the amplitude of the detected signal at the same time. A photomultiplier tube (PMT) (R7400U-20 Hamamatsu, Japan) was used to detect fluorescence signal due to its high sensitivity. A 65 dB RF amplifier was used to amplify the output signal of the PMT. To effectively eliminate the excitation light, two cascaded band-pass filters (830 nm, MK Photonics, Albuquerque, NM) were used on the detection site. A collimation system based on two aspherical lenses (Newport Corporation, CA) was designed to achieve maximum filtering efficiency. The HIFU transducer (H102, Sonic Concepts, Inc., WA) with a center frequency of 1.1 MHz was mounted on a xyz translational stage and used to generate focused hot spot. The lateral full width half maximum (FWHM) of the focal spot was 1.33 mm. The transducer was driven by a sinusoidal signal generated by a functional generator (PTS 500, Programmed Test Sources, Inc., WA) and amplified by a power amplifier (200L, Amplifier Research, Inc., PA).

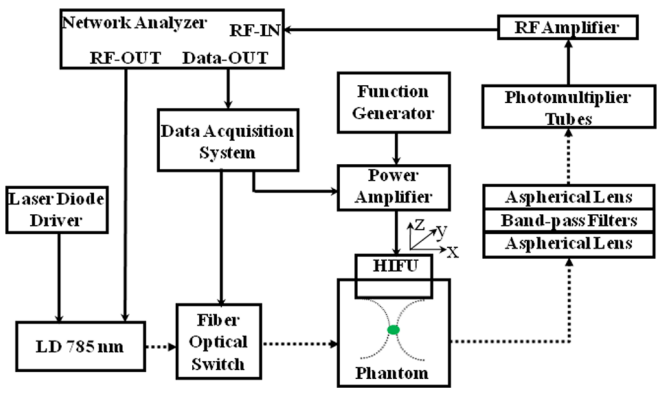

FIG. 1. (Color online) The schematic diagram of the TM-FT system. The HIFU transducer is driven by a combination of a signal generator and an RF power amplifier. Using a xyz translational stage, it is scanned over the probed medium that is simultaneously irradiated with modulated laser light. The intensity variations are detected using a photomultiplier tube and measured by a Network Analyzer.

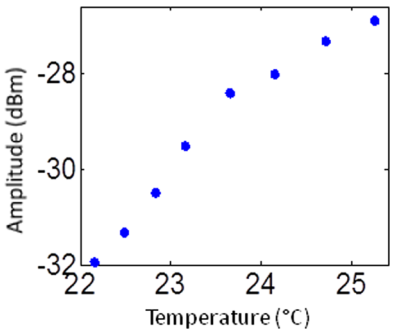

FIG. 2. (Color online) Temperature response of Pluronic ICG. The amplitude signal is recorded with the network analyzer, and the temperature is measured using a fiber optical temperature sensor.

The temperature sensitive agent Pluronic ICG was provided by our collaborator from Innosense. LLC. In order to verify the responsiveness of pluronic-ICG to temperature increase, we recorded the fluorescence intensity and the contrast agent solution temperature at the same time. The pluronic-ICG is placed in a 1 cm wide cuvette, and the fluorescence intensity was measured using the photomultiplier tube with source and detector fibers placed in orthogonal directions. A fiber-optic temperature sensor (FTC-DIN-ST-GE, Photon Control, Inc., BC, Canada) was inserted in the cuvette to monitor the temperature while heating it using a thermoelectric cooler. The amplitude signal increased around 5 dB (intensity increases 1.8 times) as the temperature increases only 3-4 °C as shown in Fig. 2, indicating an increased ICG fluorescence yield.

The experimental set up is shown in Fig. 3. A 4 cm × 10 cm × 10 cm slab gel phantom made from agarose is immersed in a water tank. The HIFU transducer is mounted on a xyz translational stage and placed on top of the phantom. The transducer is scanned laterally in both x and y directions. The measurement at each scan position is averaged four times, which yields 2 s acquisition time for each point. In order to know the point spread function (PSF) of

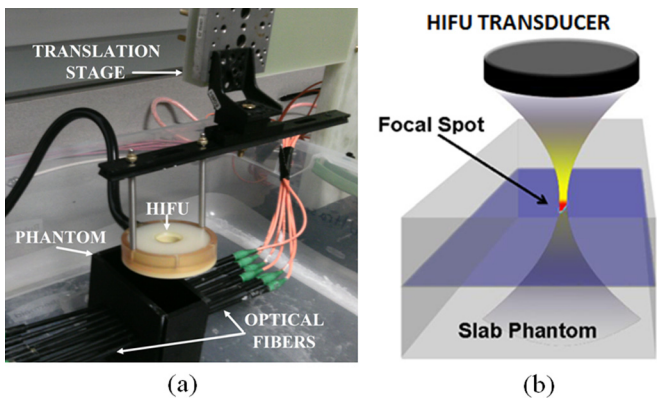

FIG. 3. (Color online) Experimental set-up. (a) The picture of the system. The HIFU transducer is mounted on an xyz translation stage. The source and detector fibers are placed in opposite side of the phantom to acquire fluorescence measurements in transmission mode. (b) The diagram of the transducer zoom-in view. During the HIFU scan, a localized temperature increase on the focal spot (~1.5 mm size) is generated. As a result, the measured fluorescence signal only changes when the focal spot is on the fluorescence source.

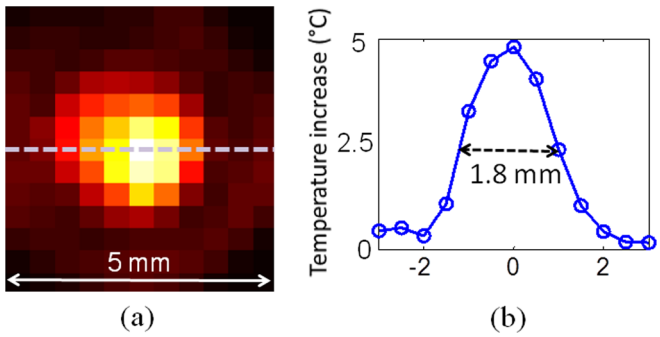

FIG. 4. (Color online) The point spread function measurement. (a) An optical temperature sensor is inserted in the phantom and the temperature change is recorded when the HIFU is scanned through a 5 mm × 5 mm area with 0.5 mm steps. (b) The profile shows that the FWHM of the heating spot size is 1.8 mm.

the temperature profile generated by the HIFU, the fiber-optic temperature sensor is inserted in an agarose phantom and the temperature change is recorded when the HIFU is scanned through a 5 mm × 5 mm area with 0.5 mm steps. The normalized temperature increase in each scanning point is shown in Fig. 4(a). The profile across the sensor tip (Fig. 4(b)) shows the temperature increase as a function of x-position of the HIFU scan step. The FWHM of the heating spot size is 1.8 mm that corresponds to point spread function of our system, which in turn becomes the spatial resolution limitation for this set-up.

A 3 mm fluorescence inclusion filled with Pluronic-ICG (Innosense Inc.) is embedded in the middle of the phantom. Intralipid (0.5%) and Indian Ink are added as scatterer and absorber, making the scatter and absorption coefficient of the phantom $0.6\,\mathrm{mm}^{-1}$ and $0.005\,\mathrm{mm}^{-1}$, respectively. The actual size, position, and concentration of the inclusion are shown in Figs. 5(a) and 5(b). Firstly conventional FT measurements are acquired. Fig. 5(c) shows the conventional FT reconstruction.[11,12] A region of interest is determined from this image ($\mathrm{ROI_{TM}}$) and then the HIFU is scanned through it (8 mm × 8 mm area) with 0.5 mm steps, Fig. 5(d). For each step, the HIFU power is turned on for 2 s, and the resulting temperature in the inclusion is kept below 40 °C. The fluorescence signal variation is mapped to each scanning position, and significant change is observed only when the HIFU hot spot is scanned through the fluorescence object (Fig. 5(e)), resulting in a much improved spatial resolution. The comparison of the experimentally measured fluorescence intensity change and those predicted by the theoretical model is shown in Fig. 5(f). Excellent agreement between the theory and the experiment is obtained for this case. There is some deviation observed, which is likely attributed to the contribution of residual heating from the previous scanning step. The profiles plot across the fluorescence source for the true object and the object recovered from the TM-FT is shown in Fig. 5(f). The FWHM of the recovered object size from the TM-FT is 3.2 mm, which is really close to 3.0 mm true object size.

In this study, we have observed the temperature modulated fluorescence signal in scattering medium with HIFU resolution. This technique combines the high sensitivity of fluorescence molecular imaging and high spatial resolution of ultrasound to overcome the ill-posedness of the fluorescence tomography in scattering medium. In the past, there has been extensive effort to improve the resolution of FT. One approach is to integrate FT with other anatomic imaging modalities such as x-ray, MRI, and ultrasound.[11,13–17] However, the weakness of this approach is that it does not perform well if the fluorescent target cannot be localized in the anatomical image. The low modulation efficiency and extremely low signal to noise ratio make the implementation of ultrasound modulation of fluorescence signals difficult.[3,4] Meanwhile, an intriguing combination of optical and ultrasound techniques has led the development of photo-acoustic tomography (PAT) that can provide the optical absorption maps with much higher resolution (~1 mm) and a depth

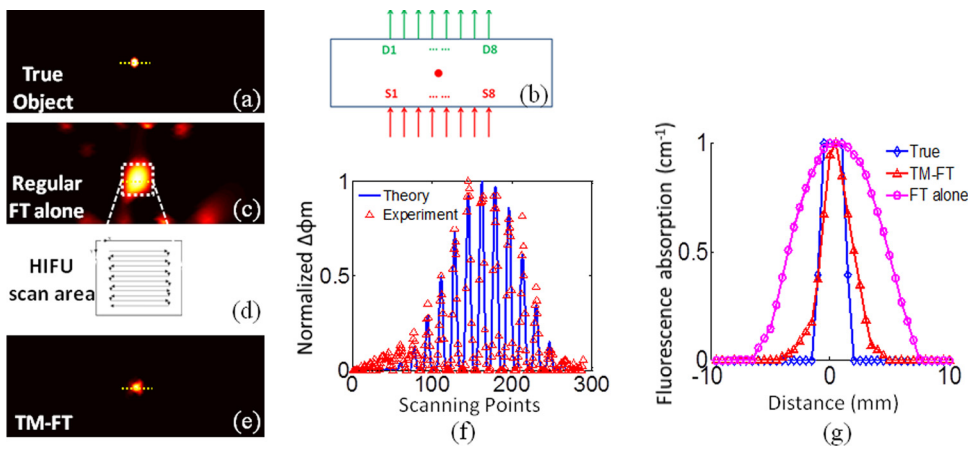

FIG. 5. (Color online) Phantom experiment results. (a) The true size and position of inclusion is shown. (b) The position of the sources and detectors is indicated in 'S' and 'D' numbers. They are placed in opposite side of the phantom to acquire fluorescence measurements in transmission mode. (c) The reconstructed fluorescence map using conventional fluorescence tomography. Meanwhile, the scanning area is determined as indicated by dashed lines. (d) The HIFU transducer is scanned through an 8 mm × 8 mm area while fluorescence measurements are taken. (e) The fluorescence signal only significantly changes when the HIFU hot spot is scanned through the fluorescence object, which reveals the high resolution fluorophore distribution map. (f) The comparison of the experimentally measured fluorescence intensity change and those predicted by the theoretical model. The theoretical prediction is shown in solid lines, while the experimental data is plotted in triangles. (g) The normalized profiles plot across the fluorescence source shows that the size of the fluorescence source is accurately recovered.

penetration of 3 to 5 cm.[1,18,19] PAT has been applied to recover spatially resolved tissue intrinsic contrast maps with very high resolution. Recently, it has demonstrated to provide distribution of exogenous contrast agents using multiple-wavelength measurements,[20–22] and an enhanced contrast of PAT signal is achieved through fluorescence quenching.[23] However, PAT is inherently sensitive to absorption and detects differential increase in absorption due to molecular probes compared to background absorption. In contrast, the TM-FT method that we have demonstrated here is directly sensitive to the fluorescence contrast. Besides obtaining fluorescence images at focused ultrasound resolution, the TM-FT can also render quantitatively accurate images using a proper reconstruction algorithm. This will be an avenue that we will pursue in the near future.

This research is supported in part by the National Institutes of Health (NIH) grants R01EB008716, R01CA142989, R21/33CA120175, R21CA121568, and by Susan G. Komen Foundation post-doc training grant: KG101442.

[1]H.-I. Wu and L. V. Wang, *Biomedical Optics: Principles and Imaging*, 1st ed. (Wiley-Interscience, New Jersey, 2007), p. 376.
[2]F. Leblond, S. C. Davis, P. A. Valdés, and B. W. Pogue, J. Photochem. Photobiol., B **98**(1), 77 (2010).
[3]M. Kobayashi, T. Mizumoto, Y. Shibuya, M. Enomoto, and M. Takeda, Appl. Phys. Lett. **89**(18), 181102 (2006).
[4]B. Yuan, Y. Liu, P. M. Mehl, and J. Vignola, Appl. Phys. Lett. **95**(18), 181113 (2009).
[5]C. Schutt, Proc. SPIE **8165**(1), 81650B (2011).
[6]B. Yuan, J. Biomed. Opt. **14**(2), 024043 (2009).
[7]A. L. Klibanov, Bioconjugate Chem. **16**(1), 9 (2004).
[8]A. M. Takalkar, A. L. Klibanov, J. J. Rychak, J. R. Lindner, and K. Ley, J. Controlled Release **96**(3), 473 (2004).
[9]C. Yongping and L. Xingde, Biomacromolecules **12**(12), 4367 (2011).
[10]T. Kim, Y. Chen, C. Mount, W. Gombotz, X. Li, and S. Pun, Pharm. Res. **27**(9), 1900 (2010).
[11]Y. Lin, W. C. Barber, J. S. Iwanczyk, W. Roeck, O. Nalcioglu, and G. Gulsen, Opt. Express **18**(8), 7835 (2010).
[12]Y. Lin, H. Yan, O. Nalcioglu, and G. Gulsen, Appl. Opt. **48**(7), 1328 (2009).
[13]S. C. Davis, B. W. Pogue, R. Springett, C. Leussler, P. Mazurkewitz, S. B. Tuttle, S. L. Gibbs-Strauss, S. S. Jiang, H. Dehghani, and K. D. Paulsen, Rev. Sci. Instrum. **79**(6), 064302 (2008).
[14]D. Kepshire, N. Mincu, M. Hutchins, J. Gruber, H. Dehghani, J. Hypnarowski, F. Leblond, M. Khayat, and B. W. Pogue, Rev. Sci. Instrum. **80**(4), 043701 (2009).
[15]A. Ale, R. B. Schulz, A. Sarantopoulos, and V. Ntziachristos, Med. Phys. **37**(5), 1976 (2010).
[16]Y. Lin, W. C. Barber, J. S. Iwanczyk, W. W. Roeck, O. Nalcioglu, and G. Gulsen, J. Biomed. Opt. **15**(4), 040503 (2010).
[17] J. D. Gruber, A. Paliwal, V. Krishnaswamy, H. Ghadyani, M. Jermyn, J. A. O'Hara, S. C. Davis, J. S. Kerley-Hamilton, N. W. Shworak, E. V. Maytin, T. Hasan, and B. W. Pogue, J. Biomed. Opt. **15**, 026028 (2010).
[18]M. Xu and L. V. Wang, Rev. Sci. Instrum. **77**(4), 041101 (2006).
[19]L. V. Wang, Med. Phys. **35**(12), 5758 (2008).
[20]L. Meng-Lin, O. Jung-Taek, X. Xueyi, K. Geng, W. Wei, L. Chun, G. Lungu, G. Stoica, and L. V. Wang, Proc. IEEE **96**(3), 481 (2008).
[21]D. Razansky, M. Distel, C. Vinegoni, R. Ma, N. Perrimon, R. W. Koster, and V. Ntziachristos, Nat. Photonics **3**(7), 412 (2009).
[22]R. Ma, A. Taruttis, V. Ntziachristos, and D. Razansky, Opt. Express **17**(24), 21414 (2009).
[23]W. J. Akers, C. Kim, M. Berezin, K. Guo, R. Fuhrhop, G. M. Lanza, G. M. Fischer, E. Daltrozzo, A. Zumbusch, X. Cai *et al.*, ACS Nano **5**(1), 173 (2010).